Carbazole-based compounds as photoinitiators for free radical and cationic polymerization upon near visible light illumination

Assi Al Mousawi, Ahmad Arar, Malika Ibrahim-Ouali, Sylvain Duval, Frederic Dumur, Patxi Garra, Joumana Toufaily, Tayssir Hamieh, Bernadette Graff, Didier Gigmes, et al.

Carbazole-based compounds as photoinitiators for free radical and cationic polymerization upon near visible light illumination†

Assi Al Mousawi,[a,b] Ahmad Arar,[a] Malika Ibrahim-Ouali,[c] Sylvain Duval,[d] Frédéric Dumur,*[e] Patxi Garra,[a] Joumana Toufaily,[b] Tayssir Hamieh,[b] Bernadette Graff,[a] Didier Gigmes,[e] Jean-Pierre Fouassier[a] and Jacques Lalevée*[a]

Six new carbazole based compounds (Ca1–Ca6) are synthesized and proposed as high performance photoinitiators with iodonium salt (iod) and/or an amine (EDB) for both the free radical polymerization (FRP) of acrylates and the cationic polymerization (CP) of epoxides upon near UV and visible light exposure using light emitting diodes (LEDs) @385 nm and @405 nm. Excellent polymerization initiating abilities are found and high final reactive function conversions are acquired. A full picture of the involved photochemical mechanisms is given.

1. Introduction

Many advantages of light-initiated processes are being reported compared to the conventional thermal ones.[1–5] For example, using light irradiation, quick responses would take place even at low temperatures (*e.g.* room temperature) and the polymerization occurs just in the irradiated area. In this context, plenty of conventional photosensitive systems are regularly accompanied by harmful UV light (*e.g.* Hg light).[6] Recently, the incorporation of visible light emitting diodes (LEDs)[7–10] as alternatives for UV sources allows bringing down in many cases energy consumption and ensures safer, longer, and specific wavelength selection. Hence the need for developing new photoinitiating systems (PISs) that are highly sensitive to higher wavelength irradiation and capable of initiating photopolymerization reactions even with low power light sources is still a hot topic.

In this work six new carbazole derivatives (Cas) bearing different substituents are synthesized (Ca1–Ca6 in Scheme 1).

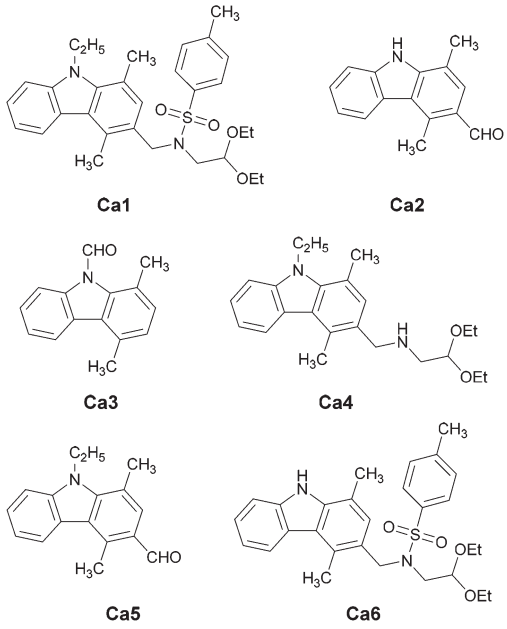

Scheme 1 The different carbazole derivatives (Cas) (noted Ca1–Ca6) investigated in this study.

They are incorporated into two-component (PI/iodonium salt Iod or PI/amine) photoinitiating systems (PISs) to induce the formation of reactive species (radicals or radical cations) for free radical polymerization (FRP) and/or cationic polymerization (CP) upon near UV or visible light LED illumination. The different substituents introduced on the carbazole scaffold will affect the absorption properties as well as the photochemical/electrochemical properties of Ca1–Ca6. In this context, different

[a]*Institut de Science des Matériaux de Mulhouse IS2M – UMR CNRS 7361 – UHA, 15, rue Jean Starcky, 68057 Mulhouse Cedex, France. E-mail: jacques.lalevee@uha.fr*
[b]*Laboratoire de Matériaux, Catalyse, Environnement et Méthodes analytiques (MCEMA-CHAMSI), EDST, Université Libanaise, Campus Hariri, Hadath, Beyrouth, Liban*
[c]*Aix Marseille Univ, CNRS, Centrale Marseille, iSm2, Marseille, France*
[d]*Unité de Catalyse et Chimie du Solide (UCCS) – UMR CNRS 8181, Université de Lille, ENSCL, Bat C7, BP 90108 59652 Villeneuve d'Ascq, France*
[e]*Aix Marseille Univ, CNRS, ICR UMR 7273, F-13397 Marseille, France. E-mail: frederic.dumur@univ-amu.fr*

reactivitives/efficiencies of carbazole derivatives in FRP and CP initiation are supposed to take place. The new photoinitiating systems will be compared to the well-known BAPO/Iod salt.

2. Experimental part

2.1. Chemical compounds

Ethyl 4-(dimethylamino)benzoate (EDB) was obtained from Sigma Aldrich (Scheme 2). Bis-(4-*tert*-butylphenyl)iodonium hexafluorophosphate (Iod or Speedcure 938) and bis(2,4,6-trimethylbenzoyl)phenylphosphine oxide (BAPO or Speedcure BPO) were obtained from Lambson. Trimethylolpropane triacrylate (TMPTA) and (3,4-epoxycyclohexane)methyl 3,4-epoxycyclohexylcarboxylate (EPOX; UVacure 1500) were obtained from Allnex and used as benchmark monomers for radical and cationic photopolymerization.

2.2. Irradiation sources

The following Light Emitting Diodes (LEDs) were used as irradiation sources: (i) LED@375 nm – incident light intensity at the sample surface: $I_0 \approx 40$ mW cm^{-2}; (ii) LED@385 nm ($I_0 \approx 120$ mW cm^{-2}); (iii) LED@405 nm ($I_0 \approx 110$ mW cm^{-2}).

2.3. Free radical (FRP) and cationic (CP) polymerization

The two-component photoinitiating systems (PISs) are mainly based on Cas/iodonium salt (1%/1% w/w) for CP and both (0.5%/1% w/w) and (1%/1% w/w) for FRP. The weight percent of the photoinitiating system is calculated from the monomer content. The photosensitive thin formulations (~25 μm of thickness) were deposited on BaF_2 pellets in air for the CP of EPOX while for the FRP of TMPTA, the formulation was sandwiched between two polypropylene films to reduce the O_2 inhibition. Excellent solubility of all carbazole derivatives was observed in EPOX and TMPTA monomers. The evolution of the epoxy group content and the double bond content of acrylate functions was continuously followed by real time FTIR spectroscopy (JASCO FTIR 4100) at about 790 cm^{-1} and 1630 cm^{-1}, respectively. The procedure used to monitor the photopolymerization profile has been described in detail in ref. 11 and 12. When a poor efficiency of the PIS is observed, low signal to noise ratios are expected.

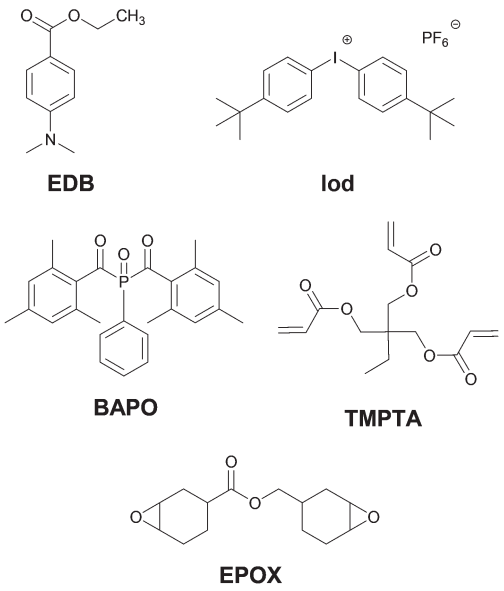

Scheme 2 Other used chemical compounds.

2.4. Redox potentials

The oxidation or reduction potentials (E_{ox} or E_{red} *vs.* SCE) for the different carbazole derivatives were measured in acetonitrile by cyclic voltammetry with tetrabutylammonium hexafluoro-phosphate (0.1 M) as the supporting electrolyte. The free energy change ΔG_{et} for an electron transfer reaction was calculated from the Rehm–Weller equation (eqn (1))[13] where E_{ox}, E_{red}, E^* and C are the oxidation potential of the electron donor, the reduction potential of the electron acceptor, the excited state energy level and the coulombic term for the initially formed ion pair, respectively. C is neglected as usually done in polar solvents.

$$\Delta G_{et} = E_{ox} - E_{red} - E^* + C \quad (1)$$

2.5. ESR spin trapping (ESR-ST) experiments, absorption experiments, fluorescence experiments, and computational procedure

The ESR-ST experiments were carried out using an X-Band spectrometer (Bruker EMX-Plus). LED@405 nm was used as the irradiation source for triggering the production of radicals at room temperature (RT) in N_2 saturated *tert*-butyl-benzene solutions, which are trapped by phenyl-*N*-*tert*-butylnitrone (PBN) according to a procedure described by us in detail.[14] The ESR spectra simulations were carried out with the PEST WINSIM program. The UV visible absorption properties of the compounds were studied using a JASCO V730 spectrophotometer (uncertainty <1%). The fluorescence properties of the compounds were studied using a JASCO FP-6200 fluorimeter.

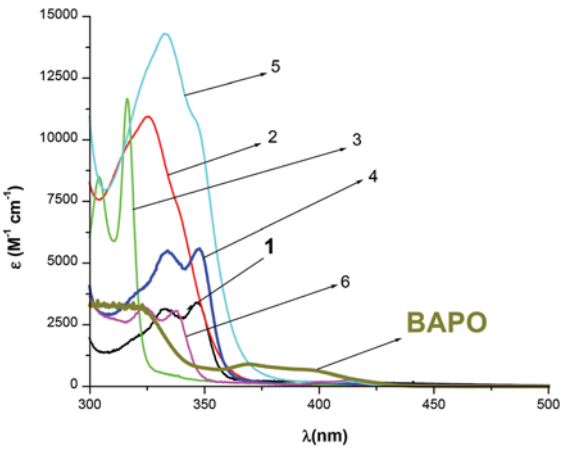

Fig. 1 Absorption spectra of the carbazole derivatives (Cas) in acetonitrile and BAPO in DCM.

Molecular orbital calculations were carried out with the Gaussian 03 suite of programs.[15,16] The electronic absorption spectra for the different compounds were calculated with the time-dependent density functional theory at the MPW1PW91/6-31 g(d) level of theory on the relaxed geometries calculated at the UB3LYP/6-31G* level of theory.

3. Results and discussion

3.1. Light absorption properties of Ca1–Ca6

The UV-visible absorption spectra of the newly proposed photoinitiators in acetonitrile are reported in Fig. 1 (see also Table 1). These compounds are characterized by high extinction coefficients in the UVA but also in the visible range (*e.g.* Ca5 ~ 14 000 M^{-1} cm^{-1} @335 nm and ~250 M^{-1} cm^{-1} @385 nm). Remarkably, their absorptions are fair in the 300–410 nm spectral range ensuring a good overlap with the emission spectra of the LEDs used in this work (*e.g.* @375 nm; @385 nm; and @405 nm) (Fig. 1).

The optimized geometries as well as the frontier orbitals (Highest Occupied Molecular Orbital (HOMO) and Lowest Unoccupied Molecular Orbital (LUMO)) are shown in Fig. 2. Both the HOMO and LUMO are strongly delocalized all over the π-system clearly showing a π → π* lowest energy transition. The presence of various substituents on the carbazole moiety causes a clear shift in the spectrum (Fig. 1).

Table 1 Absorption properties for Ca1–Ca6 *vs.* BAPO

	ε@385 nm (M^{-1} cm^{-1})	ε@405 nm (M^{-1} cm^{-1})
Ca1	~50	~50
Ca2	~120	~100
Ca3	~90	~70
Ca4	~80	~70
Ca5	~250	~210
Ca6	~70	~100
BAPO	~900	~500

3.2. Free radical photopolymerization of acrylates (TMPTA)

Among all carbazole derivatives, only Ca2 and Ca5 show very high efficiency with Iod or EDB, and the other carbazoles Ca1, Ca3, Ca4 and Ca6 show poor ability to initiate the FRP of acrylates (Table 2).

3.2.1. Carbazoles as type II photoinitiators. Carbazoles were tested as type II photoinitiators with an amine (EDB).

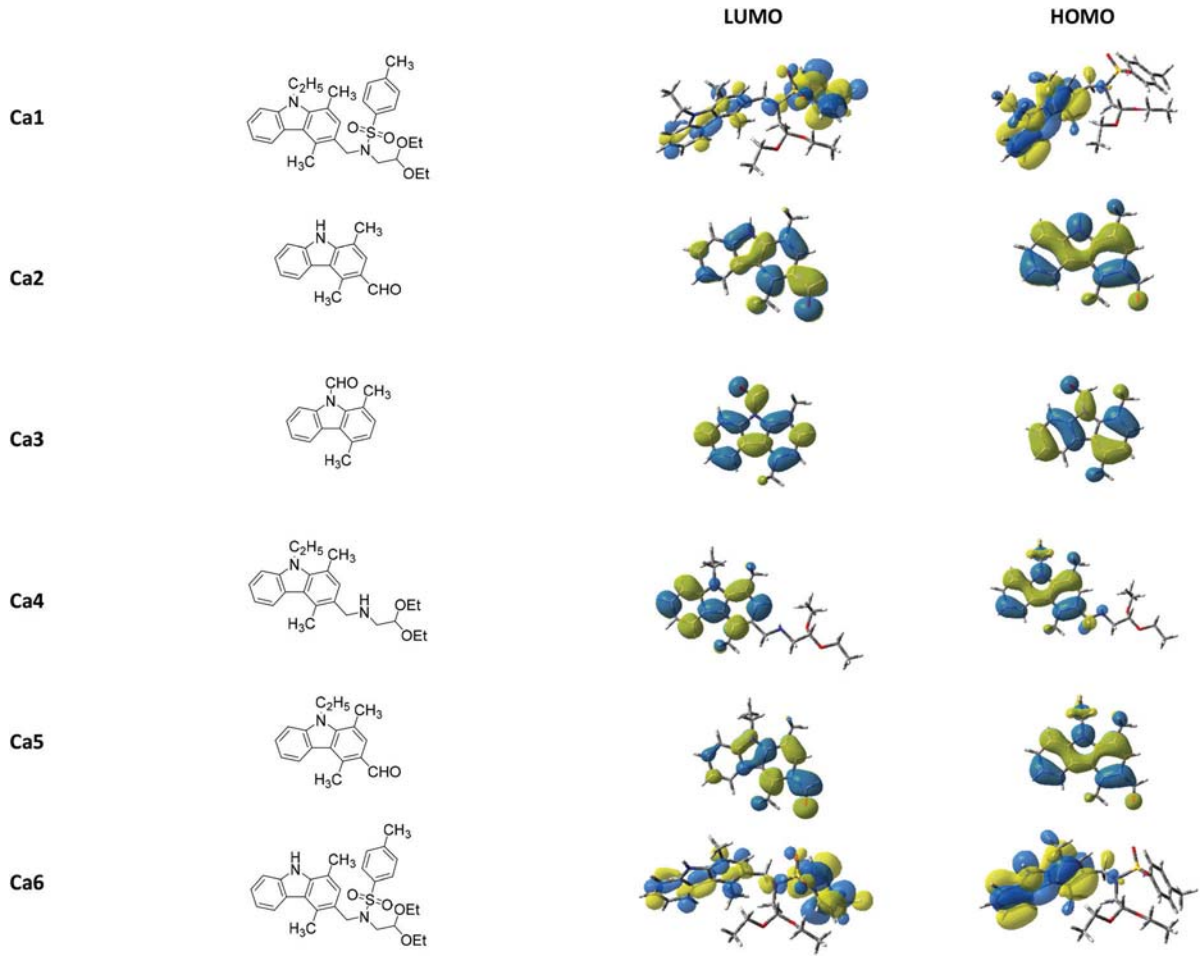

Fig. 2 Contour plots of HOMOs and LUMOs for the Cas structures optimized at the B3LYP/6-31G* level of theory.

Table 2 Final reactive function conversions (FC): epoxy for EPOX and acrylate for TMPTA using different photoinitiating systems; different LEDs for irradiation

	Epoxy function conversion FC (%) for EPOX (at t = 800 s)		Acrylate conversion FC for TMPTA (%) (at t = 400 s)			
PIS	LED@385 nm Ca/Iod (1%/1% w/w)	LED@405 nm Ca/Iod (1%/1% w/w)	LED@405 nm Ca/Iod (0.5%/1 w/w)	LED@405 nm Ca/EDB (0.5%/1% w/w)	LED@385 nm Ca/Iod (1%/1% w/w)	LED@385 nm Ca/EDB (1%/1% w/w)
Ca2	52%	39%	33%	30%	35%	52%
Ca5	54%	48%	43%	27%	50%	45%
Ca1	n.p.	n.p.	n.p.	n.p.	20%	19%
Ca3	n.p.	n.p.	15%	n.p.	20%	n.p.
Ca4	n.p.	n.p.	n.p.	n.p.	5%	27%

After irradiating a Ca/EDB system, a reaction took place between the excited state carbazoles ^{1}Ca and EDB. According to reactions (r1, r2), $EDB^{\bullet}_{(-H)}$ is formed and is responsible for the initiation of FRP. At the beginning, an electron is transferred from EDB to carbazole (r1), followed by hydrogen abstraction (r2) leading to the formation of $EDB^{\bullet}_{(-H)}$ radicals responsible for initiating FRP. These reactions are well known in the literature[1] and our results are fully compatible.

$$^1\mathrm{Ca} + \mathrm{EDB} \rightarrow \mathrm{Ca}^{\bullet -} + \mathrm{EDB}^{\bullet +} \rightarrow \mathrm{EDB}^{\bullet}_{(-H)} + \mathrm{H}^+ \qquad (r1, r2)$$

The FRP of TMPTA in thin films (25 μm) (sandwiched between two polypropylene films to avoid oxygen reaction with $EDB^{\bullet}_{(-H)}$ ketyl radicals) in the presence of the different Ca/EDB (0.5%/1%EDB w/w) couples is efficient using LED@405 nm, while EDB alone, or Ca alone cannot initiate FRP. This shows that carbazole derivatives are efficient as type II photoinitiators in photoreduction processes (electron transfer from EDB to Ca) to initiate a FRP. Typical acrylate function conversion–time profiles are given in Fig. 3A and the FCs are summarized in Table 2. High FCs are reached in Ca2/EDB and Ca5/EDB systems (*e.g.* Ca2/Iod FC = 30% at t = 400 s; Fig. 3A, curve 2 using LED@405 nm). However, upon using higher intensity LED@385 nm and a higher concentration of carbazole derivatives in Ca/EDB PIS (1%/1% w/w), the efficiency of carbazoles is much more better. The efficiency in FRP using LED@385 nm is rather higher for Ca2/EDB and Ca5/EDB than with LED@405 nm (*e.g.* Ca2/Iod FC = 52% at t = 400 s; Fig. 3B, curve 2). The efficiency trend of carbazole derivatives as type II photoinitiators upon using LED@385 nm follows the following order: Ca2 > Ca5 > Ca4 ≅ Ca1 ≅ Ca3 ≅ Ca6. The better light absorption properties of Ca2 and Ca5 derivatives (Table 1) are responsible for the higher reactivity. Similarly, upon using LED@405 nm, the efficiency trend of carbazole derivatives follows the same trend already seen above with LED@385 nm.

3.2.2. Carbazoles as photosensitizers. Carbazoles were tested as photosensitizers with iodonium salt. In fact, the Ca/Iod interaction corresponds to an electron transfer reaction finally leading to an aryl radical $Ar^{\bullet}$ (r3) and (r4). $Ar^{\bullet}$ is considered as the initiating species for the radical polymerization:

$$\mathrm{Ca} \rightarrow {}^1\mathrm{Ca}\ (h\nu) \qquad (r3)$$

$$^1\mathrm{Ca} + \mathrm{Ar_2I^+} \rightarrow \mathrm{Ca}^{\bullet +} + \mathrm{Ar_2I}^{\bullet} \rightarrow \mathrm{Ca}^{\bullet +} + \mathrm{Ar}^{\bullet} + \mathrm{ArI} \qquad (r4)$$

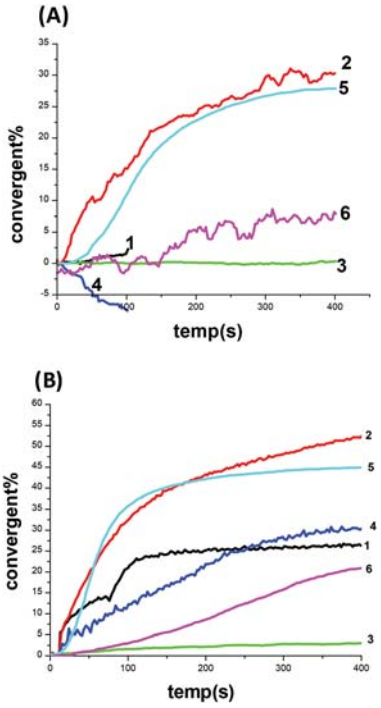

Fig. 3 (A) Polymerization profiles of TMPTA (acrylate function conversion *vs.* irradiation time) sandwiched between two polypropylene films upon exposure to LED@405 nm in the presence of: (1) Ca1/EDB (0.5%/1% w/w); (2) Ca2/EDB (0.5%/1% w/w); (3) Ca3/EDB (0.5%/1% w/w); (4) Ca4/EDB (0.5%/1% w/w); (5) Ca5/EDB (0.5%/1% w/w); and (6) Ca6/EDB (0.5%/1% w/w). (B) Polymerization profiles of TMPTA (acrylate function conversion *vs.* irradiation time) sandwiched between two polypropylene films upon exposure to LED@385 nm in the presence of: (1) Ca1/EDB (1%/1% w/w); (2) Ca2/EDB (1%/1% w/w); (3) Ca3/EDB (1%/1% w/w); (4) Ca4/EDB (1%/1% w/w); (5) Ca5/EDB (1%/1% w/w); and (6) Ca6/EDB (1%/1% w/w).

The FRP of TMPTA in thin films (laminate) in the presence of the different Ca/Iod couples is efficient using LED@405 nm, while Iod alone or Ca alone cannot initiate the polymerization (*e.g.* Ca5/Iod FC = 43% at t = 400 s; Fig. 4A, curve 5 using LED@405 nm). However, upon using higher intensity LED@385 nm and a higher concentration of carbazole derivatives in Ca/Iod PIS (1%/1% w/w), the efficiency of carbazoles is much more better. In fact, carbazole derivatives are quite efficient in photo-oxidation processes (electron transfer from Ca to Iod) to initiate a FRP in combination with Iod. Typical

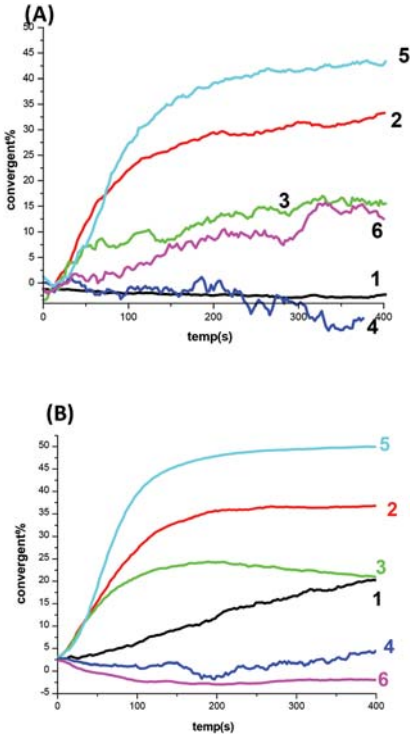

Fig. 4 (A) Polymerization profiles of TMPTA (acrylate function conversion *vs.* irradiation time) sandwiched between two polypropylene films upon exposure to LED@405 nm in the presence of: (1) Ca1/Iod (0.5%/1% w/w); (2) Ca2/Iod (0.5%/1% w/w); (3) Ca3/Iod (0.5%/1% w/w); (4) Ca4/Iod (0.5%/1% w/w); (5) Ca5/Iod (0.5%/1% w/w) and (6) Ca6/Iod (0.5%/1% w/w). (B) Polymerization profiles of TMPTA (acrylate function conversion *vs.* irradiation time) sandwiched between two polypropylene films upon exposure to LED@385 nm in the presence of :(1) Ca1/Iod (1%/1% w/w); (2) Ca2/Iod (1%/1% w/w); (3) Ca3/Iod (1%/1% w/w); (4) Ca4/Iod (1%/1% w/w); (5) Ca5/Iod (1%/1% w/w) and (6) Ca6/Iod (1%/1% w/w).

acrylate function conversion–time profiles are given in Fig. 4A, B and the FCs are summarized in Table 2. High FCs are reached in C/Iod systems (*e.g.* Ca5/Iod FC = 50% at t = 400 s; Fig. 4B, curve 5 using LED@385 nm).

In comparison with BAPO/Iod (0.5%/1% w/w),[17] carbazoles have more or less the same behaviour with slight superiority of BAPO/Iod PIS.

The efficiency trend of carbazole derivatives as photosensitizers upon using LED@385 nm follows the following order: BAPO > Ca5 > Ca2 > Ca6 ≅ Ca1 ≅ Ca3 ≅ Ca4. The better light absorption properties of Ca2 and Ca5 derivatives (Table 1) are responsible for the higher reactivity. Similarly, upon using LED@405 nm, the efficiency trend of carbazole derivatives follows more or less the same trend already seen above with LED@385 nm.

3.3. Cationic photopolymerization (CP) of epoxides

Carbazoles were tested as photoinitiators with iodonium salt (Iod). In fact, upon Ca/Iod interaction, an electron transfer reaction occurs finally leading to the formation of a carbazole radical cation $C^{\bullet+}$ responsible for CP initiation ((r3) and (r4) see above). Among all carbazole derivatives, only Ca2 and Ca5 show very high efficiency, and the other carbazoles Ca1, Ca3, Ca4 and Ca6 show poor ability to initiate CP with Iod salt (Table 2).

Upon LED@385 nm irradiation, the CP of epoxides (*e.g.* EPOX) in air using two-component photoinitiating systems based on Ca/Iod combinations (1%/1% w/w) exhibits a high efficiency in terms of final epoxy function conversion (FC) (*e.g.* FC 54% with Ca5 and 52% with Ca2; Fig. 5A, curves 1 and 3, Table 2). However, upon using a safer irradiation source *i.e.* LED@405 nm, lower efficiency compared to that upon using LED@385 nm is found (*e.g.* with LED@405 nm, FC 48% with Ca5 and 39% with Ca2; Fig. 5A, curves 2 and 4, Table 2). This

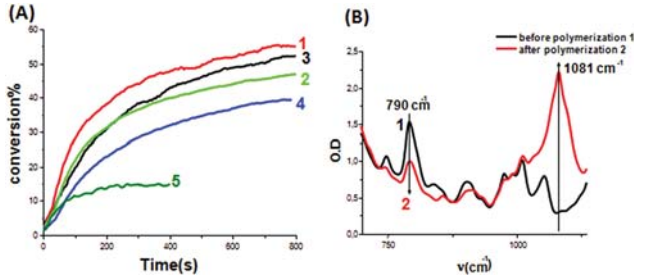

Fig. 5 (A) Polymerization profiles of EPOX (epoxy function conversion *vs.* irradiation time) upon exposure in air to: LED@385 nm in the presence of different photoinitiating systems: (1) Ca5/Iod (1%/1% w/w); (3) Ca2/Iod (1%/1% w/w); (5) BAPO/Iod (0.5%/1% w/w) and to LED@405 nm in the presence of different photoinitiating systems: (2) Ca5/Iod (1%/1% w/w); (4) Ca2/Iod (1%/1% w/w); (5) BAPO/Iod (0.5%/1% w/w). (B) IR spectra recorded before and after polymerization using Ca5/Iod (1%/1%w/w).

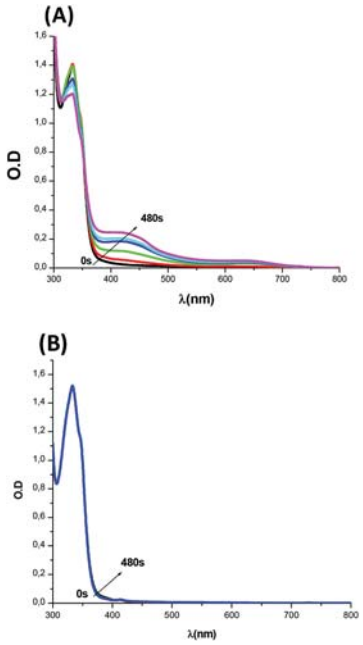

Fig. 6 (A) Ca2/Iod photolysis upon exposure to LED@375 nm and (B) photolysis of Ca2 in the absence of Iod.

is related to the fact that LED@385 nm is a more powerful irradiation source and has a higher light intensity compared to LED@405 nm. A new peak ascribed to the polyether network arises at ~1080 cm^{-1} (Fig. 5B) in the FTIR spectra. Iod alone does not activate the polymerization clearly showing the role of a radical cation which is responsible for CP initiation. Remarkably, high rates of polymerization (Rp) were clearly achieved with the Ca5/Iod system compared to the BAPO/Iod system set as a reference for which almost no polymerization occurs. In comparison with a well-known BAPO/Iod (1%/1% w/w) system, Ca2 and Ca5 are found to be much better photoinitiators than BAPO (Fig. 5, curve 5 for BAPO compared to curve 2 for Ca5 and curve 4 for Ca2 with LED@405 nm). These data show the extreme superiority of the new carbazoles Ca2 and Ca5 in terms of efficiency over the well-known BAPO.

The efficiency trend for CP using LED@385 nm follows the order: Ca5 > Ca2 > BAPO > Ca6 ~ Ca1 ~ Ca3 ~ Ca4. Obviously, this is directly related to the absorption properties of the carbazole derivatives as Ca5 is the leader in the efficiency trend and has a higher extinction coefficient at 385 nm compared to the others (see light absorption properties).

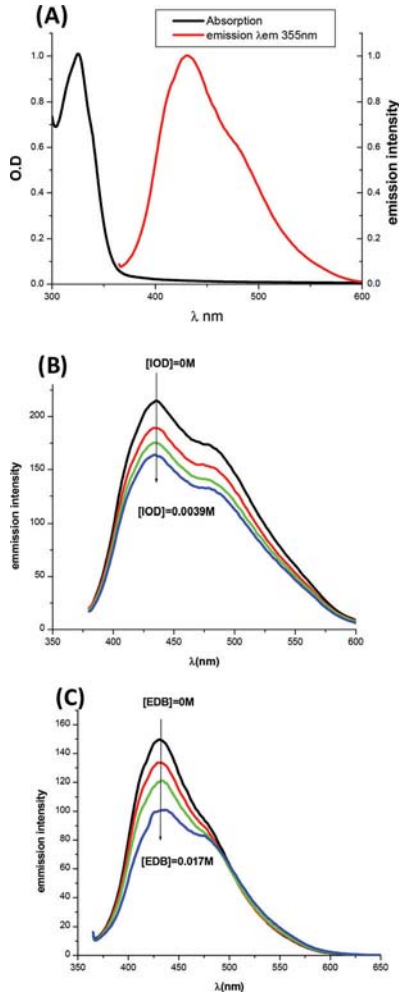

Fig. 7 (A) Singlet state energy determination; (B) fluorescence quenching of ^{1}Ca2 in the presence of Iod. (C) Fluorescence quenching of ^{1}Ca2 in the presence of EDB.

3.4. Photochemical mechanisms

The study will be focused on one of the carbazole derivatives Ca2 due to its high efficiency.

3.4.1. Steady state photolysis. The steady state photolysis of Ca2/Iod in acetonitrile is very fast compared to the high photostability of Cas alone (*e.g.* Ca2/Iod in Fig. 6A *vs.* Ca2 alone in Fig. 6B). A new photo-product (characterized by a significant new absorption for λ > 400 nm) is formed due to the Ca2/Iod interaction. Two clear isosbestic points are shown in Fig. 6A showing that no side reaction occurs.

3.4.2. Fluorescence quenching, cyclic voltammetry CV, and electronic spin resonance ESR. Fluorescence tests of Ca2 (as an example) in acetonitrile are shown in Fig. 7. The crossing point of the absorption and fluorescence spectra leads to the determination of the first singlet excited state energies (E_{S1}) (*e.g.* estimation of E_{S1} for Ca2: ~3.53 eV; Table 3, Fig. 7A).

As a mark for the occurrence of interactions, fast fluorescence quenching processes of Ca2 by Iod or by EDB are noted (*e.g.* fluorescence quenching of ^{1}Ca2 in the presence of Iod (Fig. 7B), and fluorescence quenching of ^{1}Ca2 in the presence of EDB (Fig. 7C); Table 3). The oxidation or reduction potentials of Ca2 were determined by cyclic voltammetry (CV) (*e.g.* in Fig. 8A and B). All these data (E_{ox}, E_{red}, E_{S1}), allow the calculation of free energy changes $\Delta G_{et}{}^1$ for reaction (r2) with EDB or (r4) with Iod arising from S_1 from the classical Rehm–Weller equation (eqn (1)). These processes from S_1 are found favorable *e.g.* Ca2 with Iod ΔG_{etS1} = −1.79 eV and Ca2 with Iod ΔG_{etS1} = −0.55 (eV) (Table 3). The phenyl radicals (Ar$^\bullet$), formed upon Ca/Iod interaction (r4) and responsible for FRP initiation, were easily detected as PBN/Ar$^\bullet$ radical adducts in

Table 3 Parameters characterizing the chemical mechanisms associated with the Ca2, Ca5, and Ca6/Iod; EDB systems in acetonitrile

	$E_{ox}{}^a$ [V]	$E_{red}{}^a$ [V]	E_{S1} [eV]	$\Delta G_{etS1}{}^b$ [eV]	$E_{T1}{}^c$ [eV]	$\Delta G_{etT1}{}^b$ [eV]	K_{sv} (M^{-1})	$\Phi_{et(S1)}$
Ca2/Iod	1.36		3.53	−1.79			81.9	0.33
Ca5/Iod	1.07		3.23	−2			70	0.35
Ca6/Iod	1.14		3.54	−1.9			87.66	0.4
Ca2/EDB		−1.7	3.35	−0.55			27.55	
Ca5/EDB			3.23				29.06	

[a] Oxidation or reduction potentials for Ca2, Ca5, and Ca6. [b] Reduction potential of −0.2 V (ref. 1) is used for Iod; oxidation potential of 1.1 V (ref. 1) is used for EDB in eqn (1). [c] From molecular orbital calculations (uB3LYP/6-31G* level of theory).

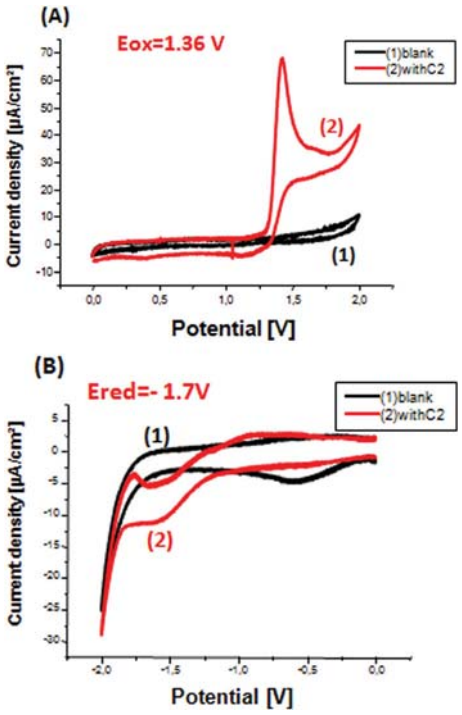

Fig. 8 (A) Cyclic voltammetry for the Ca2 oxidation; (B) cyclic voltammetry for the Ca2 reduction.

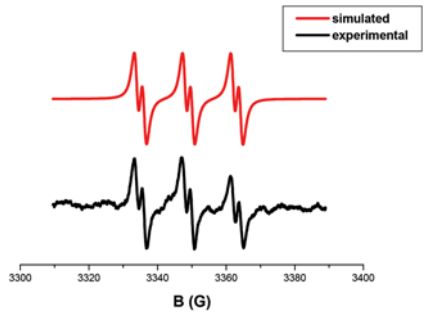

Fig. 9 ESR-ST spectra obtained upon irradiation (LED@405 nm) of Ca2/Ar_2I^+, experimental (bottom spectrum), and simulated (top spectrum) in *tert*-butyl-benzene as a solvent.

the irradiated Ca/Iod systems in ESR-ST experiments (*e.g.* for the Ca2/Iod system in Fig. 9). Indeed, the simulation of the experimental ESR spectrum yields the hyperfine coupling constants (hfcs): a_N = 14.05 G and a_H = 2.16 G typical of the PBN/Ar$^\bullet$ radical adducts.[18] This supports the occurrence of the reactions (r4) and the generation of the $PI^{+\bullet}$ radical cation responsible for the ring opening of EPOX in the presence of the two-component systems.

Conclusions

In the present paper, carbazole is proposed as an interesting scaffold for the development of a new high performance photoinitiator upon near UV or visible light exposure using LEDs for the photoinitiation of both the cationic polymerization of epoxides and the free radical polymerization of acrylates. Remarkably, Ca2 and Ca5 can be considered as new high performance photoinitiators. High final conversions and polymerization rates are obtained (for multifunctional monomers), and upon comparison with the well-known BAPO as a photoinitiator, it is found that the new carbazole derivatives are better cationic photoinitiators.

Acknowledgements

The authors thank the "Agence Nationale de la Recherche" (ANR) for the grant "FastPrinting".

Notes and references

1 J.-P. Fouassier and J. Lalevée, *Photoinitiators for Polymer Synthesis, Scope, Reactivity, and Efficiency*, Wiley-VCH Verlag GmbH & Co.KGaA, Weinheim, 2012.
2 J.-P. Fouassier, *Photoinitiator, Photopolymerization and Photocuring: Fundamentals and Applications*, Hanser, Cincinnati, Gardner Publications, New York, 1995.
3 K. A. Dietliker, *Compilation of Photoinitiators Commercially Available for UV Today*, Sita Technology Ltd, Edinbergh, London, 2002.
4 S. Davidson, *Exploring the Science, Technology and Application of UV and EB Curing*, Sita Technology Ltd, London, 1999.
5 M. A. Tasdelen, G. Yilmaz, B. Iskin and Y. Yagci, *Macromolecules*, 2012, **45**, 56–61.
6 J. H. Lee, R. K. Prud'Homme and I. A. Aksay, *J. Mater. Res.*, 2001, **16**, 3536–3544.
7 J.-P. Fouassier and J. Lalevée, *Photochemistry*, 2015, **42**, 215–232.
8 F. Dumur, D. Gigmes, J.-P. Fouassier and J. Lalevée, *Acc. Chem. Res.*, 2016, **49**, 1980–1989.
9 C. Dietlin, S. Schweizer, P. Xiao, J. Zhang, F. Morlet-Savary, B. Graff, J.-P. Fouassier and J. Lalevée, *Polym. Chem.*, 2015, **6**, 3895–3912.
10 N. Zivic, M. Bouzrati-Zerelli, A. Kermagoret, F. Dumur, J.-P. Fouassier, D. Gigmes and J. Lalevée, *ChemCatChem*, 2016, **8**, 1617–1631.
11 J. Lalevée, N. Blanchard, M.-A. Tehfe, M. Peter, F. Morlet-Savary, D. Gigmes and J.-P. Fouassier, *Polym. Chem.*, 2011, **2**, 1986–1991.
12 J. Lalevée, N. Blanchard, M.-A. Tehfe, M. Peter, F. Morlet-Savary and J.-P. Fouassier, *Macromol. Rapid Commun.*, 2011, **32**, 917–920.
13 D. Rehm and A. Weller, *Isr. J. Chem.*, 1970, **8**, 259–271.

14 J. Lalevée, N. Blanchard, M.-A. Tehfe, F. Morlet-Savary and J.-P. Fouassier, *Macromolecules*, 2010, **43**, 10191–10195.
15 J. B. Foresman and A. Frisch, *Exploring Chemistry with Electronic Structure Methods*, Gaussian. Inc., Pittsburgh, PA, 15106 USA, 2nd edn, 1996.
16 M. J. Frisch, G. W. Trucks, H. B. Schlegel, G. E. Scuseria, M. A. Robb, J. R. Cheeseman, V. G. Zakrzewski, J. A. Montgomery, J. R. E. Stratmann, J. C. Burant, S. Dapprich, J. M. Millam, A. D. Daniels, K. N. Kudin, M. C. Strain, O. Farkas, J. Tomasi, V. Barone, M. Cossi, R. Cammi, B. Mennucci, C. Pomelli, C. Adamo, S. Clifford, J. Ochterski, G. A. Petersson, P. Y. Ayala, Q. Cui, K. Morokuma, P. Salvador, J. J. Dannenberg, D. K. Malick, A. D. Rabuck, K. Raghavachari, J. B. Foresman, J. Cioslowski, J. V. Ortiz, A. G. Baboul, B. B. Stefanov, G. Liu, A. Liashenko, P. Piskorz, I. Komaromi, R. Gomperts, R. L. Martin, D. J. Fox, T. Keith, M. A. Al-Laham, C. Y. Peng, A. Nanayakkara, M. Challacombe, P. M. W. Gill, B. Johnson, W.-M. Chen, W. Wong, J. L. Andres, C. Gonzalez, M. Head-Gordon, E. S. Replogle and J. A. Pople, *Gaussian 03, Revision B-2*, Gaussian, Inc., Pittsburgh PA, 2003.
17 A. A. Mousawi, D. M. Lara, G. Noirbent, F. Dumur, J. Toufaily, T. Hamieh, T.-T. Bui, F. Goubard, B. Graff, D. Gigmes, J.-P. Fouassier and J. Lalevée, *Macromolecules*, 2017, **50**, 4913–4926.
18 J. Lalevée, M.-A. Tehfe, A. Zein-Fakih, B. Ball, S. Telitel, F. Morlet-Savary, B. Graff and J.-P. Fouassier, *ACS Macro Lett.*, 2012, **1**, 802–806.